Energy, Environmental and Technical Assessment for the Incorporation of EAF Stainless Steel Slag in Ceramic Building Materials

Rosendo J. Galán-Arboledas[a,*], Javier Álvarez de Diego[a], Michele Dondi[b], Salvador Bueno[a,c]

[a] Fundación Innovarcilla, Pol. Ind. El Cruce, C/ Los Alamillos 25, 23710. Bailén (Jaén), Spain

[b] Istituto di Scienza e Tecnologia dei Materiali Ceramici, CNR-ISTEC, Via Granarolo 64, 48018. Faenza, Italy

[c] Departamento de Ingeniería Química, Ambiental y de los Materiales. Campus Científico Tecnológico de Linares, Universidad de Jaén, Cinturón sur s/n, 23700, Linares (Jaén). Spain.

*Corresponding author. Tel.: +34 953 67 85 59. Fax: + 34 953 67 85 60

E-mail address: *tecnico@innovarcilla.es*

Abstract

The paper studies the addition of electric arc furnace stainless steel (EAF-SS) slag to clay raw materials for ceramic brick manufacturing in order to get more sustainable materials without compromising their final properties. Different amounts (10 wt.%, 20 wt.% and 30 wt.%) of EAF-SS slag were added to a reference clay material. The samples were processed by extrusion and the main technological properties were determined to characterize the behavior of the materials during the shaping and drying processes (working moisture, drying linear shrinkage and modulus of rupture) and the final properties of sintered materials (bulk density, linear shrinkage, water absorption and modulus of rupture) at five maximum temperatures (850, 900, 950, 1000 and 1050 ºC). The environmental impact was evaluated by qualitatively analyzing gaseous emissions during firing and by leaching tests on laboratory specimens. Furthermore, energy demand and fuel (natural gas) required to produce the formulated compositions,

according to a standard industrial scale, was calculated in both the dryer and the kiln. Calculation of CO_2 emissions during such theoretical industrial processing was also performed. Results show that the incorporation of EAF-SS leads in general to adequate technological properties and causes a potential saving of up to 17 % of natural gas consumption and a reduction in CO_2 emissions of up to 24 % during manufacturing materials with 30 wt.% of EAF-SS slag at 950 ºC. However, in these materials the higher metals leaching potential would restrain the EAF-SS slag incorporation to a content of about 10 wt.% or less and to sintering temperatures >950 °C. Therefore, clay ceramics incorporating EAF-SS slag in their composition can be technologically feasible and environment-friendly depending on both sintering temperature and amount of waste addition.

Keywords: EAF stainless steel slag, ceramic building materials, energy demand, environmental assessment, technology properties.

1. Introduction

The construction sector is one of the pillars of the development of the global economy at the expense of being one of the principal actors in the consumption of energy and materials. In particular, building materials affect the environment throughout their whole life cycle, from the extraction of raw materials until the products arrive at landfill as construction waste, through the stages of manufacturing, construction and use of the buildings. Specifically, the energy used for the extraction of raw materials and manufacture of the building materials (embodied energy), together with emissions at these stages, represents a significant fraction of the environmental impact caused by construction materials during their life cycle [Giama and Papadopoulos, 2015; Zabalza-Bribián et al., 2011]. So, recent reviews [Eco-Innovation Observatory, 2011] show that there is a shift in the ratio between operational and embodied carbon, that it is now becoming closer to 60:40 for an average building and with a trend for the embodied contribution to become the dominating factor in the future.

In this context, the ceramic bricks and roof tiles, refractories and wall and floor tiles sub-sectors together emitted a total of 19 Mt CO_2 in 2010. Of these emissions, 66% were due to fuel combustion, with electricity and process emissions accounting for 18% and 16% respectively [Cerame-Unie, 2012]. However, it should be noted that the use of ceramic building materials based in fired clay presents a number of advantages compared to other materials because they require less maintenance cost, they are very resistant materials with chemical inert nature, 100% inorganic, and with high durability (up to 150 years) and resistance to weathering. The energy consumption and emissions during the manufacturing process of ceramic materials make them apparently less competitive in terms of environmental impact unless maintenance cost, durability and re-use are concerned [Cerame-Unie, 2012; TBE, 2014].

To reduce the environmental impact associated with the production of ceramics, the introduction of wastes as alternative raw materials for the ceramic industry is especially viable with the aim of energy and materials savings [Raut et al., 2011; Zhang, 2013]. This is possible due to the peculiar features of the ceramic manufacturing process, that includes a firing step at high temperatures (>850 ºC) that allows the waste to release its calorific value during the sintering process, if an organic nature residue is added, [Demir, 2008; Barbieri et al., 2013] or to be incorporated into the internal structure of ceramics if an inorganic one is used [Alonso-Santurde et al., 2011; Binhussain et al., 2014; Gencel et al., 2013; Mymrin et al., 2014].

In particular, inorganic wastes such as steel slag are massively generated in Europe mainly from two types of primary furnaces in steelmaking industries: basic-oxygen furnace (BOF) and electric-arc-furnace (EAF) that are usually followed by a ladle furnace for further steel refining (Euroslag). The latter two processes (EAF and ladle) account for around 25% of slag production in Europe, according to data from 2012, and are especially relevant in the case of Spain, where most of the steel is produced from EAF with subsequent refining [Unesid, 2014]. In this regard, since 13 % of the steel slag continue to be disposed in landfill, different experiences of EAF-SS slag valorisation have been described in the scientific literature, mainly related to their use in civil engineering and cement production because the great production of this waste would be only recoverable by the industry of building materials and the construction sector in general [Candian-Lobato et al., 2015; Yi et al., 2012], although a previous recovery of heavy valuable metals is recommended or necessary [Huaiwei and Xin, 2011; Kim et al., 2016]. Also valorisation in the manufacture of ceramics for building (bricks and tiles) has been analysed showing EAF-SS slag a composition generally compatible with common clays, as demonstrated by several studies on the use of this type of waste as alternative raw material for the manufacture of a variety of ceramic products [Cunico et al., 2003; Sarkar et al., 2010; Shih et al., 2004; Teo et al., 2014; Zhao et al., 2015].

However, most of these studies on EAF-SS slag recovery do not evaluate the modification of energy demand and CO_2 emissions associated with the manufacturing of ceramic materials that incorporate this kind of waste in their composition. This information is essential for a rigorous environmental impact assessment [Almeida et al., 2015; Díaz Rubio and Del Río Merino, 2014; Koroneos and Dompros, 2007; TBE, 2014] and for the quantification of benefits associated with the valuation of certain waste. Therefore, the current work is intended to fill this gap by a preliminary calculation of the energy demanded by a standard clay brick manufacturing process incorporating a typical slag obtained from EAF-SS production, along with the amount of fuel required to produce these ceramics and the CO_2 emissions associated with fuel combustion and materials sintering reactions. The discussion of the results has been related to a basic materials technological characterization that includes both the behaviour of materials during the manufacturing steps and their final performance.

2. Materials and Methods

2.1. Raw Materials

A traditional clay mixture from Comercial Cerámicas de Bailén (Jaén, Spain) was used as reference material for comparison. This reference clay mixture is encoded as R, and it has been described in Galan-Arboledas et al. (2013) as a common formulation used by the brickmaking industry for the manufacture of ceramic products for partition walls. Electric arc furnace slag from refined stainless steel production, encoded as EAF-SS, or just SS for simplicity in Tables and Figures, was supplied by the waste management company FCC-Ámbito once de-metallized and crushed. Therefore, the waste was provided as a sand (80 wt.% of particles with a grain size between 125 and 800 μm, measured by direct sieving, Table 1) and only scattered aggregates showed a maximum size of the order of 0.5-1 cm. Real density of both clay and slag was determined by He

picnometry (Accupyc II 1340, Micromeritics, USA). Increasing amounts of EAF-SS slag (10 wt.%, 20 wt.% and 30 wt.%) were added into the reference material R in order to formulate RSS10, RSS20 and RSS30 compositions.

2.2. Characterization Methods

2.2.1. Clay and Waste Composition. The chemical composition of the reference clay formulation, R, was determined by energy dispersive X-ray fluorescence spectrometry (PANalytical, Axios PW4400, The Netherlands), with scintillation and flow detectors and rhodium anode (Rh), while the mineralogical composition was determined by XRD (X-ray diffraction, Bruker, D8I-90, USA) with Bragg-Brentano configuration and geometry θ:θ, Cu anticathode and standard conditions of speed 2° 2θ/min at 30 kV and 40 mA, on both bulk sample and oriented aggregates for the fraction <2μm. A semi-quantitative identification of mineral phases was carried out by the classic method of diffraction peak area measurement and reflection power [Schultz, 1964]. In the case of EAF-SS slag, the chemical composition was determined by wavelength dispersive X-ray fluorescence spectrometry (PANanalytical, Axios Advanced, The Netherlands) using a rhodium tube (Rh) with voltage 4 kW. The mineralogical analysis was performed with a Bruker D8 Advance, in the 10-80°2Θ range with 1 s per step and LynxEye0.02º 2Θ detector. The qualitative identification of mineral phases took place from Powder Diffraction File references (PDF2 Release 2009).

In addition, water-soluble fraction of EAF-SS slag was determined by dispersing 10 g of sample in 200 ml of deionized water, keeping under stirring for 24 h and then separating the solid by filtration. The solution obtained was dried at 105°C and the dry residue was weighed, expressing the result as a percentage of starting sample. In turn, the dry residue was analyzed by XRPD for the quantitative determination of the constituent phases of efflorescence [Dondi et al., 1997a].

2.2.2. Processing and Technology Properties. Since EAF-SS slag was provided as sand with scattered aggregates, both the starting clay, R, and the slag were first dry ground together in a hammer mill (Royal Triumph, H6300/1, Spain) with a sieve of 3 mm. Then batches were shaped by extrusion adding an amount of water sufficient to achieve a consistency of 1.8 kg/cm^2, as measured with pocket penetrometer (Tascabili, ST 207, Italy). Shaping was performed in a laboratory extruder (Verdés, Monobloc 050-C/OR, Spain) at 90% vacuum. Dimensions of obtained test bars were 120 x 28 x 18 mm^3. The green and dry specimens were characterized by measuring Working Moisture and Drying Shrinkage, determined by differential weighing and length, respectively, after a drying process in a forced air oven at 105 ± 5°C until constant mass and length. Modulus of Rupture (MOR) was obtained from a three-point bending strength test (HOYTOM, CM-C, Spain) using a load cell of 5 kN, 100 mm span and a displacement rate of 10 mm/min. Reported results are the mean value and standard deviation of four determinations for Working Moisture and Drying Shrinkage, while MOR was obtained as the mean value of six determinations.

Dynamic sintering studies in static atmosphere were performed by thermal dilatometric analysis, using a horizontal dilatometer (Linseis, L76/1400, Germany) and by thermogravimetric and differential scanning calorimetry, TG-HDSC, (Linseis, STA PT1600, Germany) up to a maximum temperature of 1050°C, with 10°C/min as heating and cooling rates. Firing of test specimens was carried out in a laboratory electric furnace (KITTEC CB, CBN-50, Germany) at five maximum temperatures: 850, 900, 950, 1000 and 1050°C for 3 hours dwell, with a heating rate of 4°C/min up to 400°C, 2°C/min up to 700°C and 1°C/min up to the maximum temperature, while the cooling was performed at 4°C/min down to 600ºC, 2°C/min down to 400°C and 4°C/min down to room temperature. Selected firing temperatures and heating/cooling rates are usual at industrial scale for manufacturing common ceramic bricks for partition walls (850ºC-950ºC) and facing bricks and roof tiles (950ºC-1050ºC).

Fired specimens were characterized by Bulk Density (determined by mercury immersion displacement), Water Absorption (UNE-EN ISO 10545-3) as an indirect measurement of open porosity, and MOR (as described above for dry materials, but with a displacement rate of 5 mm/min). Reported results are the mean value and standard deviation of three determinations for Bulk Density, Linear Firing Shrinkage and Water Absorption, while MOR was obtained as the mean value and standard deviation of six determinations.

2.2.3. Environmental Impact I: Leaching test. In order to assess the leachate degree in the ceramic materials, fired specimens were analyzed by leaching test under the methodology established in the standard EN 12457-2 (2002) and taking the limit values set by European Council (2002) for deposition of non-hazardous waste in landfill. According to this legal decision, metals analysed were Cr, Ni, Cu, Zn, As, Se, Mo, Cd, Sb, Ba, and Pb, by using distilled water for 24 hours as extractive medium and a liquid to solid ratio L/S=10. Metals determination was performed with an ICP-Mass instrument (Agilent, 7500a, USA).

2.2.4. Environmental Impact II: Energy consumption assessment. The energy needed to manufacture the materials under investigation was calculated in order to assess the change in fuel demand that the introduction of EAF-SS slag may induce during industrial production at 950 ºC. For this calculation, an energy balance was carried out, both in the dryer and the furnace.

First, it was calculated the energy involved in the drying process, which aims to evaporate the water added for shaping. In this preliminary study, it was only taken into account the energy consumption required to vaporize the water present in the wet bodies and, therefore, it has been obviated for simplicity other energy consumptions associated mainly with heating of the pieces and losses inside the dryer facilities, as well as other factors such as temperature and humidity of the air used in the drying itself [Alvarez de

Diego et al., 2012; Massaguer and Amposta, 2015]. These parameters depend on the particular type of dryer, so for a preliminary comparison between materials is assumed that these factors are similar for the different studied compositions. Thus, the enthalpy to dry the ceramic material, H_d, in Megawatts (MW) was calculated by Equation (1) according to a basic energy balance.

$$H_d = Q_{ds} \cdot WM \cdot H_{VH_2O} \quad (1)$$

Where Q_{ds} is the inlet mass flow into the dryer, expressed as dry solid material per second ($kg_{Dry\ Solid}/s$), WM is the working moisture per unit (kg_{H2O} / $kg_{Dry\ Solid}$) and H_{vH2O} is the vaporization enthalpy for water (2.5 MJ/kg_{H2O}).

Secondly, the energy involved in the process of material sintering was simplified as a reaction to transform the raw materials into the final ceramic product. As described above for the drying process, other contributions to energy consumption during the firing process have not been considered for a preliminary comparison between the different compositions. Thus, sintering reaction energy was calculated by Equation (2) according to basic thermodynamics.

$$H_r = Q_{KS} \cdot C_s \cdot 10^{-3} \quad (2)$$

Where H_r is the sintering reaction enthalpy in MW, Q_{KS} is the inlet mass flow into the ceramic kiln expressed as dry solid material per second ($kg_{Dry\ Solid}/s$) and C_s is the specific heat capacity (J/g). Determination of C_s was carried out by thermogravimetric and differential scanning calorimetry, TG-HDSC (Linseis, STA PT1600, Germany) in order to obtain mass loss and endothermic and exothermic reactions in the different compositions at a heating rate of 10°C/min up to 950°C, using platinum crucibles and sapphire as

standard. To determine the values of C_s in selected temperature ranges the software Win-STA (Linseis) has been used.

From the process enthalpy values ($H_{d,r}$), calculation of fuel used in both the drying and the sintering process was carried out through and energy balance with Equations (3-4):

$$H_{d,r} = H_f = Q^o_{fd,r} \cdot LCV_f \quad (3)$$

$$Q^o_{fd,r} = \left(H_{d,r}/LCV_f\right) \cdot 10^3 \quad (4)$$

where enthalpy or energy demanded by the process ($H_{d,r}$, in MW) is equated to the enthalpy that needs to be provided by the fuel (H_f) and $Q^0_{fd,r}$ is the flow of fuel used in the dryer (d) or the furnace (r), assuming that the fuel used is natural gas under normal conditions, whose units are Nm^3/h, and LCV_f is the natural gas lower calorific value (10,357 kWh/Nm^3). For this balance, and with a comparative purpose between different compositions, it has been considered a heat conversion efficiency of 1 for natural gas, since is assumed for simplicity the same type of installation and excess air required for proper fuel combustion. Generally, excess air required in ceramic brick kilns typically ranges between 1.1 and 1.3 and, in addition, heat losses in industrial facilities achieve up to 40 % of given energy [Alvarez de Diego et al., 2012; Massaguer and Amposta, 2016].

2.2.5. Environmental Impact III: analysis of gaseous emissions. First, a qualitative determination of the gaseous emissions during materials sintering was carried out at laboratory scale. In particular, carbon dioxide (CO_2), sulfur dioxide (SO_2), chlorine (Cl) and fluorine (F) gaseous emissions were determined by coupling a simultaneous thermal analysis equipment TG-DSC (Netzsch STA 449 C Jupiter, Germany) to a quadrupole mass spectrometer, QMS (Bruker, 403 QMS Aëolos, USA) and to a Fourier transform

infrared spectrometer, FTIR (Bruker, TGA-IR, USA). Volatile compounds emitted as HCl, CO_2 and SO_2 were determined by QMS, through their corresponding relations m/z (36, 44 and 64 respectively) while HF emissions were determined by FTIR. The analyses were performed up to a maximum temperature of 1050 °C with a heating rate of 10 ºC/min in a dynamic atmosphere of air (flow rate of 50 mL/min) and helium as shield gas (25 mL/min).

Then, once studied the qualitative emission of gas compounds, CO_2 emissions associated with fuel combustion (Equation 5) and carbonates content (Equation 6) were calculated according to regional legislation by the methodology used in the Support Guide for Reporting PRTR (Pollutant Release and Transfer Register) in the Manufacturing Industry of Ceramic Building Elements [Junta de Andalucía, 2014].

$$CO_2 Emissions Fuel = Q_{fd,r}^{O} \cdot \rho_f \cdot LCV_f \cdot EF \cdot OF \qquad (5)$$

Where $Q_{fd,r}^{O}$ is the fuel consumed during the drying and firing in Nm^3/h, ρ_f is the fuel density (0.8 Kg/Nm^3), LCV_f is the natural gas lower calorific power (48.28 MJ/Kg), EF and OF are emission and oxidation factors whose values are 0.056 Kg CO_2/MJ and 0.995, respectively. These CO_2 emissions due to fuel consumption are expressed in Kg/h.

$$CO_2 Emissions Carbonates = Pd \cdot [Carb] \cdot 0.44 \qquad (6)$$

Where P_d is the daily production of the furnace in Kg/h, [Carb] is the carbonates percentage content determined by the standard UNE 130200 (1993), and 0.44 is the emission factor from calcium carbonate expressed in Kg CO_2/Kg carbonate. The CO_2 emissions due to carbonates decomposition are expressed in Kg/h.

For extrapolating the obtained results to a typical brickmaking factory, a production of 300 and 250 ton/day was considered for the drying and firing step respectively. A common duration of 6 and 7 days a week for running the drier and furnace, respectively, was also considered.

3. Results and Discussion

3.1. Characterization of Raw Materials

The chemical composition of the reference clay, R, and the EAF-SS slag is shown in Table 2. Clay R is characterized by a high content of SiO_2 and CaO, with significant amounts of Al_2O_3 and Fe_2O_3, highlighting the presence of K_2O as a fluxing agent. On the other hand, EAF-SS slag is rich in CaO and SiO_2, but with reversed proportions with respect to R, accompanied by significant contents of Al_2O_3, MgO, Cr_2O_3 and MnO, while the Fe_2O_3 content is very low. This composition is consistent with that of described EAF-SS slag [Shih et al., 2004; Yi et al., 2012; Yildirim and Prezzi, 2011], with CaO and SiO_2 as major constituents. A peculiarity of the studied EAF-SS slag is the minor content of Fe and the presence of Cr_2O_3 associated to high-alloy refined stainless steel compositions as described in [Huaiwei and Xin, 2011; Kim et al., 2016].

Since the relatively high Chromium content in the slag (2.8 wt.% Cr_2O_3, Table 2) can be a potential hindrance for its valorization in the manufacture of ceramic materials, it is necessary to determine the Chromium oxidation state. However, taking into account that the XRPD analysis of the slag soluble fraction (only 0.2 wt.% of the sample) is made up of uncolored calcite and bassanite, it can be hypothesized that the Chromium oxidation state is Cr^{3+}. Therefore, its stability during the sintering process of ceramic specimens will depend on the furnace atmosphere and the mineralogical phase where Chromium is allocated [Dondi et al., 1997b]. If Cr is incorporated into the structure of Ca-Mg silicates

(akermanite and/or merwinite) it is expected to be retained as Cr^{3+}, but if dissolved in the vitreous phase, it will be likely oxidized to Cr^{6+}, especially if firing reactions occur with alkaline elements [Xu et al., 2005], as highly probable once the slag is dispersed in the clay matrix. Therefore, in order to establish the degree of metals stabilization, including Chromium, in the proposed clay-slag fired compositions, leaching test have been performed and main results are analyzed in paragraph 3.3.1.

On the other hand, XRD analyses of raw materials are shown in Figure 1 and phase semi-quantification is summarized in Table 3. The phyllosilicate fraction of the reference material R is characterized by illite and smectite prevailing over kaolinite (Table 3). This composition is suitable for brick industrial processing, since the presence of smectite in the clay confers greater plasticity, facilitating extrusion forming, while the presence of illite and feldspars also ensures a relatively high fluxing character, thus generating liquid phase during the heat treatment, which allows consolidating the material in the subsequent cooling and increasing its mechanical strength [Barba et al., 2002]. In addition, the carbonates content (calcite and dolomite, Table 3) as well as quartz amount are adequate to promote a porous microstructure typical of ceramic bricks for partition walls due to firing transformations (Fabbri and Dondi, 1995). Furthermore, the EAF-SS slag is mainly composed of calcium and magnesium silicates like merwinite (30-40 wt.%) and akermanite (20-30 wt.%), in agreement with reported phases for EAF-SS slag [Kim et al., 2016; Huaiwei and Xin, 2011; Yi et al., 2012; Yildirim and Prezzi, 2011] but with the difference that no Fe compounds are detected due to the low content of this element. Other phases present in the steel slag in lower proportions are calcite and quartz (5-10 wt.%) being the amorphous/vitreous component in an intermediate proportion (10-20 wt.%) as indicated by the presence of a small “hump” at low 2θ angle (5°-20°) in the XRD pattern (Figure 1). Therefore, a lack of plasticity is expected from this slag composition.

3.2. Technological Properties of Ceramic Body

3.2.1. Characterization on Green and Dry Bodies

The main technological properties characterized on green and dry bodies are listed in Table 4. These values show that increasing EAF-SS slag contents induced a decrease in the Working Moisture necessary for shaping, at the same consistency, according to the plasticity reduction expected from slag incorporation. The decreasing Working Moisture also involves a diminution of Drying Linear Shrinkage, because this contraction is due to the elimination of water used for shaping.

It can also be observed that increasing the EAF-SS slag proportion in the mixture decreased the MOR (Table 4). This MOR decline is also related to the lower plasticity of slag-bearing compositions. In fact, plasticity is a characteristic property of clay minerals (phyllosilicates, Table 3) on which molding of clay-water mixtures is based [Moore, 1965] and, in particular, it is highly dependent on particle size. In this sense, phyllosilicates, especially smectites, are fine-grained materials (< 2 μm) and thus they are responsible for the increased fine particle fraction in the starting clay R compared to EAF-SS (fraction < 125 μm, Table 1). Therefore, the MOR of the samples increased when the clay content increased in the studied mixtures. Furthermore, the slag particle size may also influence the MOR, because having a particle size distribution different from that of clay causes a different particle packing during forming, which can reduce the mechanical strength [Barba et al., 2002].

3.2.2. Sintering Studies

When clay is fired at high temperatures, it experiences permanent and irreversible changes that give place to a complete modification of its properties. Thus the characteristics of the fired material differ from those of the starting one in size, structure and composition, resulting, in general, a hard material, resistant to water and chemicals. Thus, the main reactions taking place during the thermal treatment of the R clay and the

slag-bearing compositions proposed in this work are illustrated in Figure 2. Between room temperature and 500°C, the thermo-dilatometric curves (Fig. 2a) show a continuous dilation of the batches, whereas in calorimetric curves (Fig. 2c) two endothermic peaks appear related to moisture loss (~100ºC) and removal of characteristic interlayer water of smectite (~170ºC) [Merino et al., 2007]. These endothermic peaks match with the weight loss shown in thermogravimetric curves up to ~220 ºC (Fig. 2b). Above 200°C, oxidation of organic matter gave place to an exothermic peak in the DSC curves whose maximum intensity occurs between 300 °C and 450 ºC.

From 500 to 600 ºC the DSC curves show the allotropic transformation of α-quartz to β-quartz as an endothermic peak at 573ºC (Fig. 2c) [González-García et al., 1988; Barba et al., 2002]. A weight loss is also produced from ~500°C (Fig. 2b) related to the de-hydroxylation of the phyllosilicates present in the clay [Merino et al., 2007; Barba et al., 2002]. Above 600°C, the thermal expansion proceeded at a slower rate (Fig. 2a) up to temperatures around 770-780°C for the different compositions, at which the clay-slag mixtures underwent their maximum dilatation. This maximum expansion occurred during the decomposition of carbonates, shown as an endothermic peak in the DSC curves (Fig. 2c) and a weight loss in the TGA curves (Fig. 2b) [Barba et al., 2002; González-García et al., 1988; Merino et al., 2007]. This weight loss is greater in the clay than in the mixtures, being indicative of the lower carbonates content of the starting mixtures incorporating slag (Calcite and Dolomite, Table 3).

After the temperature of maximum expansion, a strong shrinkage began in all mixtures (Fig. 2a) due to an internal rearrangement governed, at least in part, by liquid phase sintering and reactions occurring between CaO and the clay matrix [Dondi et al. 1999]. Free CaO at these temperatures comes from previous carbonates decomposition (Calcite + Dolomite) according to reactions: $CaCO_3 \rightarrow CaO + CO_2\uparrow$ and $CaMg(CO_3)_2 \rightarrow CaO + MgO + 2CO_2\uparrow$). This shrinkage stopped at ~920°C, temperature at

which a new expansion occurred until the final test temperature, 1050ºC, associated to exothermic peaks in the DSC curves (Fig. 2c). According to the starting compositions (Table 2 and 3) such transformations from 920 ºC can be hypothesized to be caused by the formation of Ca-Mg crystalline phases [Barba et al., 2002; Fabbri and Dondi, 1995; González-García et al., 1988; Serra et al., 2014]. However, a XRD analysis would be necessary in order to determine which newly formed crystalline phases exactly they were. These analyses are currently underway to characterize the mineralogy of the sintered ceramic products. Regarding the thermogravimetric curves (Fig. 2b), once the carbonates decomposition finished, no change in mass was observed for the reference clay; however, for mixtures incorporating EAF-SS, a very slight mass gain occurred, likely due to oxidation of some compounds present in the slag [Shih et al., 2004].

3.2.3. Characterization of Sintered Materials

The evolution of the main technological properties in the firing range 850-1050 ºC is shown in Figure 3. It can be seen how the addition of EAF-SS slag in the clay R caused an increase in bulk density of the mixtures, except at 1050°C, when R has a density greater than RSS10 and RSS20. This fact is due to the faster sintering rate of the clay, which has the highest shrinkage at that temperature, as shown in the dilatometric curves (Fig. 2a). Furthermore, the waste-bearing compositions are expected to have increased open porosity as shown indirectly through the values of water absorption capacity (Fig. 3) and in agreement with trends reported by Shih et al. (2004). These higher values of both bulk density and water absorption in the slag-bearing bricks are apparently contradictory, but it is the effect of the high specific weight of EAF-SS slag with respect to clay (real density, Table 1).

Regarding the MOR values, the slag-bearing mixtures have lower values than reference clay R (Figure 3), as reported by Shih et al. (2004) at similar firing temperatures. This is

the result of two converging factors: the slag is in starting coarser grains (Table 1), that can play as weakness point in the final microstructure, and it has an inert behavior (as the slag is a mainly crystalline product from a high-temperature process, it is inert to the sintering process if temperature is not high enough) that favors the higher porosity in these materials. Both the coarser grains and the porosity contribute weakening the structure. However, at all events, the MOR values are within common reported values for masonry products (Fabbri and Dondi, 1995).

These general trends can be better understood by analyzing the evolution of technological properties with firing temperature. The mixtures incorporating EAF-SS slag experienced an increase of MOR values from 950ºC upward. This increase is greater for the mixtures incorporating higher slag amounts, although the water absorption capacity of these materials remained unchanged or increased slightly, contrary to what occurred in the clay R, in which water absorption capacity decreased at 1050ºC. Thus, the increase in mechanical strength of the waste-bearing compositions can be attributed mainly to the contribution of crystalline phases development instead of melting and vitreous phase formation [Dondi et al., 1999; González-García et al., 1988; Serra et al., 2014]. In fact, the behavior of the mixtures is typically a refractory one (according to ceramic terminology) since the values of properties such as bulk density and water absorption capacity remain stable with increasing the sintering temperature due to the evolution of crystalline phases and pore size, which caused the increasing MOR [Serra et al., 2014]. As described above, further studies are currently underway to determine the newly formed crystalline phase in the sintered ceramic product.

3.3. Environmental Impact

3.3.1. Leaching Tests. Leaching tests were carried out on the materials RSS10 and RSS30 sintered at 850 ºC, 950 ºC and 1050 ºC, as an indirect way to check whether the chemical elements that compose the EAF-SS slag were completely inertized within the

ceramic matrix. The analyzed leaching elements (Cr, Ni, Cu, Zn, As, Se, Mo, Cd, Sb, Ba, Pb and Hg) were chosen according to European Legal Decision for controlling deposition of non-hazardous waste in landfill [European Council, 2012]. The results in Table 5 show that only Cr and Mo exceeded the limits established by the Council Decision. Cr exceeds the maximum permitted leaching limit of 10 mg/kg in the RSS30 sintered at 850, 950 and 1050 ºC, with values of 33.5, 30.9 and 75.1 mg/kg respectively. The increase of Cr leachate concentration with temperature is in contrast with the general trend of clay bricks, as observed for reference clay R, where Cr is increasingly immobilized for firing temperatures from 800 to 1000°C [Dondi et al. 1997b] and presumably due to the oxidation behavior of the steel slag [Shih et al., 2004]. In contrast, the RSS10 values of 11.8 and 10.1 mg/kg of Cr leachate were found after firing at 850 and 950ºC, respectively, and thus very close to the threshold. In the case of Mo, the leaching limit (10 mg/kg) is overpassed (12.6 mg/kg) only in the mixture RSS30 sintered at 1050°C (Table 5).

To summarize, values exceeding widely the threshold are not systematic, but limited to the higher amount of slag (RSS30 composition); this implies that bricks made up of 30 wt.% slag are environmentally not feasible. Other cases are just over the limit of 10 mg/kg, i.e. a release in the order of 0.5% of total Cr present in the body (Table 1). The occurrence of water soluble Cr is due to partial oxidation to chromate, a process difficult to be kept under strict control in industrial conditions. However, this inconvenience can be overcome by different technological solutions (firing curve, slag particle size, etc).

3.3.2. Energy Assessment. The energy balance taken into account in this paper considers only the inputs and outputs of energy due to material transformations (*i.e.*, evaporation of working moisture and reactions during sintering). Thus, other contributions, such as thermal energy recovery from the kiln to the dryer, the entry and exit of wagons in a typical brickmaking industrial process or energy losses through kiln

walls and roof, are not considered, since they are assumed to be the same for all materials [Alvarez de Diego et al., 2012]. In addition, the drying and sintering processes account for ~ 70-80 % of embodied energy of a typical ceramic brick and it mainly corresponds to thermal energy originated from fuels combustion [Díaz Rubio and Del Rio Merino, 2014]. The ~ 25% remaining energy is power consumption, i.e. associated to milling processes [Alvarez de Diego et al., 2012], which has not been evaluated in this study since incorporated slag is supplied already crushed and can be dried and milled together the starting clay.

Table 6 shows the energy estimation for the drying process, H_d, calculated by Equation (1), assuming it is used to evaporate the water added for extrusion (Working Moisture, Table 4). Increasing the amount of EAF-SS slag allows to decrease the amount of energy demanded to evaporate the water added, H_d, due to the reduced Working Moisture, as data in Table 4 show. This reduction in the energy demand brings about a correspondent decreasing of fuel used in the dryer, Q^0_{fd}, of around 3.2%, 8.2% and 18.7 % for RSS10, RSS20 and RSS30 materials, respectively.

After the drying study, a quantification of the energy necessary for brick sintering at 950 ºC was carried out by a series of thermal analyses in order to account the weight loss, Figure 2b, and the endothermic and exothermic reactions, Figure 2c, occurring during sintering, as described in paragraph 3.2.2. From these analyses, the curves of specific heat (C_e, Fig. 4) were calculated as a function of temperature, and subsequent divided in detailed specific ranges where the main physical-chemical transformations occur (a: loss of moisture and/or water adsorbed; b: oxidation of organic matter; c: de-hydroxylation of clay phyllosilicates and quartz allotropic transformation; d: decomposition of carbonates: e: formation of new crystalline phase). Table 7 shows the values of specific heat, C_{ex}, corresponding to the temperature intervals, ΔT_x, for such transformations, calculated as the area under the curve. Then, the sum of the specific

heat values of each interval indicates the global specific heat for the corresponding formulation to be sintered at 950°C (C_s, Table 7).

It can be seen how the global specific heat, C_s, for waste-bearing compositions decreased and therefore, by increasing the amount of EAF-SS slag, the energy involved in the sintering process is decreasing (H_r, Table 7). This reduction is mainly due to the lower carbonate content of the mixtures incorporating EAF-SS slag, which results in the decrease in the value of the specific heat, C_e, in the temperature range 630 °C – 820 °C (Figure 4, Table 7) when the carbonate decomposition takes place (Figure 2). In fact, carbonate decomposition is an endothermic process which is responsible for consuming most of the energy during the sintering process of ceramic materials [Álvarez de Diego et al., 2012]. This reduction of the energy involved in the sintering process, H_r, involves a decrease of the fuel used in the furnace, Q^0_{fr}, of approximately 2.5 %, 11.4 % and 14.0 % for RSS10, RSS20 and RSS30 materials respectively. In addition, if a standard industrial scale production is considered, with a drier production of 300 ton/day, running 6 days a week, and a kiln production of 250 ton/day, operated 7 days a week, it would involve a saving of 1068, 3199 and 6214 Nm^3 of fuel per week for RSS10, RSS20 and RSS30 compositions respectively, assuming the use of natural gas with the characteristics mentioned in paragraph 2.2.3.

3.3.3. Emissions Analysis of CO_2, SO_2, HCl and HF. A qualitative analysis of these emissions with temperature has been performed since they are the dominant gaseous emissions in brickmaking (together with CO and NO_x) [Gomez et al., 2007; González et al., 2006; Koroneos and Dompros, 2007]. Figure 5 shows the temperatures at which the CO_2, SO_2, HCl and HF release is produced during firing. Sulfur emissions as SO_2 occur between 395 and 500°C, and are due to the decomposition of pyrite, gypsum and organic matter as common minor associated phases in clays [González et al., 2006]. When the steel slag is added to the clay, the SO_2 signal intensity dramatically decreased,

presumably because the released SO_2 reacted with the calcium-rich matrix. This environmentally favorable fact can, however, involve the formation of efflorescence in sintered materials since sulfur compounds can experience subsequent recrystallization in wet environments.

The emission of chlorine (HCl) occurs in two different stages. The first one starts at 112°C and is related to chlorine molecules that are released along with the hydration water of the material, while the second stage has an emission maximum at 590°C and corresponds to the decomposition of NaCl or dehydroxylation of clay minerals. These two emission stages are also observed for fluorine (HF) but additional fluorine release starts from 950°C and 875°C for RSS20 and RSS30, respectively, and is not complete at the maximum temperature of analysis, 1050 ºC. This is consistent with the formation of F-bearing transient phases (fluorite, cuspidine) that sequestrate fluorine at intermediate temperatures and release it once they turn instable [Dehne, 1987]. Anyway, both fluorine and chlorine emissions in the waste-bearing compositions are not significant and quite similar to those of the reference clay.

The quantitatively most important emission for the manufacture of ceramics is the CO_2 release. Qualitatively this emission occurs between 200ºC and 900ºC, as shown in Figure 5, with a first interval between 200ºC and 500°C corresponding to oxidation and/or combustion of the organic matter present in the mixtures (weight loss shown in Figure 2b), while the emissions between 600ºC and 900ºC correspond to the CO_2 released during carbonates decomposition (calcite and dolomite, Table 3). By introducing waste steel slag in the reference clay a reduction in the signal intensity of CO_2 emitted occurs, Figure 5, revealing the expected reduction in emissions of these compounds due to the lower carbonates content in the mixtures.

Quantitatively, the carbonate content is 18.8 ± 0.5 wt.% and 1.0 ± 0.5 wt.% for the reference clay and the EAF-SS slag, respectively, determined by standard UNE 130200 (1993). Thus the bodies RSS10, RSS20 and RSS30 have a carbonate content of 17.0 wt.%, 15.2 wt.% and 13.5 wt.%, respectively, calculated proportionally according to the mixtures rule. Assuming for sake of simplicity that all carbonates in the mixtures are calcite, whose emission factor is 0.44 Kg_{CO2} / $Kg_{carbonate}$ [Junta de Andalucía, 2014], the CO_2 emitted by the formulated materials during the carbonate decomposition (Equation 7) is shown in Table 9. Furthermore, this Table shows CO_2 emissions associated with fuel combustion during the drying and sintering process (Equation 6) calculated by the methodology used in [Junta de Andalucía, 2014].

From data in Table 9, the reduction of CO_2 emissions associated with lower carbonate content in the waste-bearing compositions is greater than the reduction caused by saving fuel consumption (82.5 kg/h, 165.0 kg/h and 242.9 kg/h versus 15.5 kg/h, 45.7 kg/h and 90.1 kg/h for RSS10, RSS20 and RSS30 materials, respectively). In the case of an industrial plant with a drier production of 300 ton/day, running 6 days a week, and a kiln production of 250 ton/day, operated 7 days a week, a reduction of 16.4, 35.4 and 55.9 tons of CO_2 per week is achieved for RSS10, RSS20 and RSS30 batches respectively. However, it is difficult to make a direct comparison of these results with data on emissions of ceramics companies because, as described above for energy consumption, in this work some factors have been simplified and also in the industrial practice is common to recirculate heat flows between the kiln and the drier.

4. Conclusions

Manufacturing ceramic materials with the addition of EAF-SS slag into traditional clay raw materials does not present significant technological problems for industrial scale production, once a slag with the appropriate particle size distribution is provided. Furthermore, the addition of EAF-SS slag improves the behavior during the drying

process by reducing the Working Moisture needed for extrusion, thus achieving a lower shrinkage. This fact reduces the occurrence of pathologies such as cracks produced during the drying process. Although mechanical resistance decreases with respect to the reference clay, waste-bearing materials present MOR values within the standard established for the industrial handling of common pieces as bricks for partition walls (>3 MPa).

Besides the technical performance of finished products is adequate for the industrial production of common bricks for separating walls, some concerns come from the actual inertization of the slag. Although a wide range of heavy metals is efficiently incorporated in the brick matrix, Chromium leachates are in some cases over the allowed threshold (and in one single case Molybdenum too). Further work is needed to study in detail the best amount of EAF-SS slag to be incorporated into the clay and the firing temperature, because the effective inertization of steel slag in a ceramic matrix depends mostly on these two parameters along with the particle size.

The environmental impact caused by the incorporation of EAF-SS slag in clay-based ceramic materials during their manufacturing at industrial scale is reduced since they require less energy, water and clay raw materials, and emissions of greenhouse gasses such as CO_2 are diminished. In particular, the reduction of carbonate content in the waste bearing formulation leads to a decrease in both fuel consumption, since smaller amounts of fuel are needed for the endothermic decomposition reaction, and CO_2 emissions due to the decomposition itself.

The proposed methodology for optimizing clay brick formulations with EAF-SS slag can be extended to a wide range of inorganic waste compositions and to any ceramic product for building (wall and floor tiles, roof-tiles, etc.) although an in-depth study of materials

microstructure and mineralogy is necessary for a clear understanding of firing transformations.

Acknowledgement

This work is part of Keram-Eco Project [P11-TEP-7253], "Waste recovery in ceramic materials for sustainable and energy efficient building", funded by the Excellence Project Programme of Junta de Andalucía and the Spanish Ministry of Economy and Competitiveness. Clay has been provided by Comercial Cerámicas de Bailén S.L.

References

Almeida, M.I., Dias, A.C., Demertzi, M., Arroja, L., 2015.Contribution to the development of product category rules for ceramic bricks. J. Clean. Prod. 92, 206-215.

Alonso-Santurde, R., Andrés, A., Viguri, J.R., Raimondo, M., Guarini, G., Zanelli, C., Dondi, M. 2011. Technological behaviour and recycling potential of spent foundry sands in clay bricks. J. Environ. Manage.92, 994-1002.

Álvarez de Diego, J., Sáez, V., Jiménez, J., Cintas, J.M., Laguna, J.A., 2012. Energy optimization tools in ceramic materials manufacturing (Herramientas para la optimización energética en la fabricación de materiales cerámicos). Fundación Innovarcilla, Bailén. http://innovarcilla.es/investigacion/proyectos-destacados/201-efiker (accesed 17.08.16)

Barba, A., Beltrán, V., Feliu, C., García, J., Gines, F., Sánchez, E., Sanz, V., 2002. Behavior of raw materials in the various stages of ceramic processing (Comportamiento de las materias primas en las distintas etapas del proceso cerámico), in: Materias primas para la fabricación de soportes de baldosas cerámicas, 2nd Ed. Instituto de Tecnología Cerámica, Castellón, pp.195-288.

1 Barbieri, L., Andreola, F., Lancellotti, I., Taurino, R., 2013. Management of agricultural
2 biomass wastes: Preliminary study on characterization and valorisation in clay
3 matrix bricks. Waste Manage. 11, 2307-2315.
4 Binhusaain, M., Marangoni, M., Bernardo, E., Colombo, P., 2014. Sintered and glazed
5 glass-ceramics from natural and waste raw materials. Ceram. Int. 40, 3543-3551.
6 Candian Lobato, N.C., Auza Villegas, E., Borges Mansur, M., 2015. Management of solid
7 wastes from steelmaking and galvanizing processes: A brief review. Resour.
8 Conserv. Recycl. 102, 49-57.
9 Ceramie-Unie, 2012. Paving the way to 2050.The ceramic industry roadmap. Ceramie-
10 Unie A.I.S.B.L., Brussels.
11 Cunico, L., Dircetti, G., Dondi, M., Ercolani, G., Guarini, G., Mazzanti, F., Raimondo, M.,
12 Ruffini, A. & Venturi, I., 2003. Steel slag recycling in clay brick production. Tile Brick
13 Int.19, 230-232.
14 Dehne, G., 1987. Relationship between fluorine emission during firing of ceramic
15 products and the firing temperature and composition of raw material. Appl. Clay Sci.
16 2, 1-9.
17 Demir, I., 2008.Effect of organic residues addition on the technological properties of clay
18 bricks. Waste Manage. 28, 622-627.
19 Díaz Rubio, R., Del Río Merino, M., 2014. Quantification of variables that determine the
20 carbon footprint and energy embodied of structural clay products (cradle to gate with
21 options). Bol. Soc. Esp. Ceram. V. 53, 194-206.
22 Dondi, M., Fabbri B., Guarini G., Marsigli M., Mingazzini C., 1997a. Soluble salts and
23 efflorescence in structural clay products: a scheme to predict the risk of
24 efflorescence. Bol. Soc. Esp. Ceram. V. 36, 619-629.
25 Dondi, M., Fabbri, B., Mingazzini, C., 1997b. Mobilisation of Chromium and Vanadium
26 during firing of structural clay products. Ziegelindustrie Int. 50, 685-696.
27 Dondi M., Guarini, G., Raimondo, M., 1999. Trends in the formation of crystalline and
28 amorphous phases during the firing of clay bricks. Tile Brick Int. 15, 176-183.

Eco-Innovation Observatory, 2011.Embodied CO_2 versus operational CO_2, in: Resource-efficient construction. The role of eco-innovation for the construction sector in Europe. Eco-Innovation Observatory, pp. 16-17.

EN 12457-2, 2002.Characterization of waste. Leaching. Compliance test for leaching of granular waste materials and sludges.

European Council, 2002. Council Decision 2003/33/EC establishing criteria and procedures for the acceptance of waste at landfills pursuant to Article 16 of and Annex II to Directive 1999/31/EC

Euroslag. www.euroslag.com/products/ (accesed 17.08.16)

Fabbri, B., Dondi, M., 1995. Caratteristiche e diffetti del laterizio. Gruppo Editoriale Faenza Editrice S.p.A., Faenza.

Galán-Arboledas, R.J., Merino, A., Bueno, S., 2013. Use of new raw materials and industrial wastes to improve the possibilities of using ceramic materials from Bailén (Jaén, southern Spain). Mater. Construcc. 63, 553-568.

Gencel, O., Sutcu, M., Erdogmus, E., Koc, V., Cay, W., Gok, M.S., 2013. Properties of bricks with waste ferrochromium slag and zeolite. J. Clean. Prod. 59, 111-119.

Giama, E., Papadopoulos, A.M., 2015. Assessment tools for the environmental evaluation of concrete, plaster and brick elements production. J. Clean. Prod. 99, 75–85.

Gómez, M. P., Gazulla, M. F., Zumaquero, E., Orduña, M., 2007. Use of coupled TG-DSC-QMS-FTIR thermal analysis techniques in characterizating clays and ceramic compositions used in ceramic tile manufacture. Quantification of carbon compounds. Bol. Soc. Esp. Ceram. V. 46, 259-266.

González, I., Galán, E., Miras, A., 2006. Fluorine, chlorine and sulphur emissions from the Andalusian ceramic industry (Spain)—Proposal for their reduction and estimation of threshold emission values. Applied Clay Science, 32, 153-171.

González García, F., García Ramos, G., Romero Acosta, V., González Rodríguez, M., 1988. Clays used in the manufacturing of artistic tiles of Seville: Properties and

transformations during the cooking process. I. $CaCO_3$ containing materials. Bol. Soc. Esp. Ceram. V. 27, 215-223.

Huaiwei, Z., Xin, H., 2011. An overview for the utilization of wastes from stainless steel industries. Resources, Conservation and Recycling, 55, 745-754.

Junta de Andalucía, 2014. Reporting PRTR (Pollutant Release and Transfer Register) data. Epigraph 3. g. Support report guide in the manufacturing industry of ceramic building elements (Notificación de datos PRTR. Epígrafe 3.g. Guía de apoyo para la notificación de la industria de fabricación de elementos cerámicos de construcción).

Kim, E., Spooren, J., Broos, K., Nielsen, P., Horckmans, L., Geurts, R., Vrancken, K.C., Quaghebeur, M., 2016. Valorization of stainless steel slag by selective chromium recovery and subsequent carbonation of the matrix material. J. Clean. Prod., 117, 221-228.

Koroneos, C., Dompros, A., 2007. Environmental assessment of brick production in Greece. Building and Environment, 42, 2114-2123.

Massaguer, A., Amposta, S., 2015. Drying and firing techniques (I) (Técnicas de secado y cocción, I). Técnica Cerámica, 423, 214-220.

Massaguer, A., Amposta, S., 2016. Drying and firing techniques (VIII) (Técnicas de secado y cocción, VIII). Técnica Cerámica, 430, 152-157.

Merino, I., Arévalo, L.F., Romero, F., 2007. Preparation and characterization of ceramic products by thermal treatment of sewage sludge ashes mixed with different additives. Waste Manage. 27, 1829-1844.

Moore, F.R., 1965. Ceramic pastes and bodies, in: Rheology of ceramic systems. Maclaren, London, pp. 45-77.

Mymrin, V., Riberiro, R., Alekseev, K., Zelinskaya, E., Tolmacheva, N., Catai, R., 2014. Environmental friendly ceramics from hazardous industrial wastes. Ceram. Int. 40, 9427-9437.

Raut, S.P., Ralegaonklar, R.V., Mandavgane, S.A., 2011. Development of sustainable construction material using industrial and agricultural solid waste: A review of waste-create bricks. Constr. Build. Mater. 25, 4037-4042.

Sarkar, R., Singh, N., Kumar, S. D., 2010. Utilization of steel melting electric arc furnace slag for development of vitreous ceramic tiles. Bull. Mater. Sci. 33, 293-298.

Shih, P., Wu, Z., Chiang, H., 2004. Characteristics of bricks made from waste steel slag. Waste Manage. 24, 1043-1047.

Schultz, L.G., 1964. Quantitative interpretation of mineralogical composition from X-ray and chemical data for the Pierre shale. U.S. Geol. Surv. Profes. Paper 391-C, 31.

Serra, M.F., Acebedo, M.F., Conconi, M.S., Suarez, G., Aglietti, E.F., Rendtorff, N.M., 2014.Thermal evolution of the mechanical properties of calcareous earthenware. Ceram. Int. 40, 1709-1716.

TBE, 2014. TBE PCR for clay construction products. Guidance document for developing an EPD. Tile & Bricks Europe A.I.S.B.L., Brussels.

Teo, P.T., Anasyida, A.S., Basu, P., Nurulakmal, M.S., 2014. Recycling of Malaysia's electric arc furnace (EAF) slag waste into heavy-duty green ceramic tile. Waste Manage. 34, 2697-2708.

UNE 103200, 1993. Determination of carbonate content in soils (Determinación del contenido de carbonatos en los suelos).

Unesid, 2014. www.unesid.org/el-sector-mapa.php (accesed 17.08.16).

Xu, H.B., Zheng, S.L., Zhang, Y., Li, Z.H., Wang, Z.K., 2005. Oxidative leaching of a Vietnamese chromite ore in highly concentrated potassium hydroxide aqueous solution at 300 ºC and atmospheric pressure. Minerals Engineering, 18, 527-535.

Yi, H., Xu, G., Cheng, J., Wang, J., Wan, Y., Chen, H., 2012. An overview of utilization of steel slag. Procedia Environmental Sciences. 16, 791-801.

Yildirim, I.Z., Prezzi, M., 2011- Chemical, Mineralogical, and Morphological Properties of Steel Slag. Advances in Civil Engineering. Vol. 2011, Article ID 463638, 13 pages.

Zabalza Bribián, I., Valero Capilla, A., Aranda Usón, A., 2011. Life cycle assessment of building materials: Comparative analysis of energy and environmental impacts and evaluation of the eco-efficiency improvement potential. Build. Environ. 46, 1133-1140.

Zhang, L., 2013. Production of brick from waste materials. A Review. Constr. Build. Mater. 47, 643-655.

Zhao, L., Wei, W., Bai, H., Zhang, X., Cang, D., 2015. Synthesis of steel slag ceramics: chemical composition and crystalline phases of raw materials. International Journal of Minerals, Metallurgy and Materials, 22, 325-33.

TABLES

Table 1: Real density and particle size distribution of the reference material, R, and EAF-SS slag

	Real Density, g/cm3	Particle Size Distribution		
		<125 µm	125-800 µm	>800 µm
R	2.70 ± 0.01	32.2 %	38.0 %	29.8 %
SS*	3.17 ± 0.01	15.2 %	79.2 %	5.6 %

*:Particle size distribution as received

Table 2: Chemical composition (wt.%) of the reference material, R, and EAF-SS slag

	SiO_2	Al_2O_3	Fe_2O_3	MnO	MgO	CaO	Na_2O	K_2O	TiO_2	P_2O_5	Cr_2O_3	BaO	SO_3	LOI*
R	43.9	8.5	3.3	0.1	2.1	20.0	0.2	1.6	0.4	0.1	-	-	0.1	19.9
SS	33.0	9.7	0.9	1.4	7.2	39.8	0.1	0.4	1.1	0.1	2.8	0.1	0.3	2.6

*LOI: Lost on ignition

Table 3: Semi-quantitative mineralogical composition (wt.%) of the reference material, R, and EAF-SS slag, obtained from Figure 1

	Q	Fd	C	D	Y	Ph	Phyllosilicates			Co	Me	Ak	Am/v
							Es	Ill	K				
R	36	7	14	4	Tr	37	40	50	10	-	-	-	-
SS	5-10	-	5	-	-	-	-	-	-	Tr	30-40	20-30	10-20

Q: Quartz; Fd: Feldspar; C: Calcite; D: Dolomite; Y: Gypsum; Ph: Phyllosilicates; Es: Smectite; Ill: Illite; K: Kaolinite; Co: Corundum; Me: Merwinite; Ak: akermanite; Am/v: Amorphous/vitreousphase; Tr: Traces

Table 4: Main technology properties of green and dry bodies

	Working Moisture [%]	Drying Linear Shrinkage [%]	MOR [MPa]
R	22.0 ± 0.1	5.8 ± 0.1	9.1 ± 0.5
RSS10	21.3 ± 0.1	5.5 ± 0.1	7.6 ± 0.3
RSS20	20.2 ± 0.1	5.5 ± 0.1	7.3 ± 0.4
RSS30	17.9 ± 0.1	4.8 ± 0.1	6.4 ± 0.4

Table 5: Leaching test of sintered materials. Values exceeding legal limits are in bold.

	T [ºC]	Cr	Ni	Cu	Zn	As	Se	Mo	Cd	Sb	Ba	Pb
R	**850**	4,1	<0,1	<0,1	<0,1	<0,1	0,1	0,6	<0,1	<0,1	0,4	<0,1
	950	1,6	<0,1	<0,1	<0,1	<0,1	<0,1	0,9	<0,1	<0,1	0,2	<0,1
	1050	0,5	<0,1	<0,1	<0,1	<0,1	<0,1	0,8	<0,1	<0,1	0,5	<0,1
RSS10	**850**	**11,8**	<0,1	<0,1	<0,1	<0,1	<0,1	0,7	<0,1	<0,1	0,4	<0,1
	950	**10,1**	<0,1	<0,1	<0,1	<0,1	<0,1	1,1	<0,1	<0,1	0,2	<0,1
	1050	7,1	<0,1	<0,1	<0,1	<0,1	<0,1	2,1	<0,1	<0,1	0,6	<0,1
RSS30	**850**	**33,5**	<0,1	<0,1	<0,1	<0,1	0,1	1,2	<0,1	<0,1	0,5	<0,1
	950	**30,9**	<0,1	<0,1	<0,1	<0,1	<0,1	3,0	<0,1	<0,1	0,5	<0,1
	1050	**75,1**	<0,1	<0,1	<0,1	<0,1	<0,1	**12,6**	<0,1	<0,1	0,7	<0,1
Limit* [mg/Kg]		10	10	50	50	2	0,5	10	1	0,7	100	10

*: Limit established by European Council Decision 2003/33 / EC for a L/S ratio = 10

Table 6: Energy (H_d) and fuel demand (Q^o_{fd}) for drying process.

	WM [%]	Qs_s [$Kg_{Dry\ Solid}/s$]	H_d [MW]	Q^0_{fd} [Nm^3/h]	Fuel Saving	
					[Nm^3/h]	[%]
R	22.0	3.472	1.910	184.4	-	-
RSS10	21.3	3.472	1.849	178.5	5,9	3.2
RSS20	20.2	3.472	1.753	169.3	15,1	8.2
RSS30	17.9	3.472	1.554	150.0	34,4	18.7

Table 7: Specific heat (C_s), energy (H_r) and fuel demand ($Q°_{fr}$) for sintering process at 950ºC.

Interval ΔT [ºC]		R	RSS10	RSS20	RSS30
		$Ce_x\Delta T_x$ [J/g]*	$Ce_x\Delta T_x$ [J/g]*	$Ce_x\Delta T_x$ [J/g]*	$Ce_x\Delta T_x$ [J/g]*
a	T_{room}-220	103.1	98.7	95.5	110.3
b	220-450	-145.9	-79.9	-75.8	-69.9
c	450-630	27.6	32.6	24.3	19.4
d	630-820	256.7	159.3	148.6	121.9
e	820-950	-49.3	-23.3	-22.4	-16.5
$C_s = \sum_{x=a}^{x=e} Ce_x\Delta T_x$		192.2 J/g	187.4 J/g	170.2 J/g	165.2 J/g
Q_{Ks} [$Kg_{Dry\ Solid}$/s]		2.894	2.894	2.894	2.894
H_r [MW]		0.556	0.542	0.492	0.478
Q^0_{fr} [Nm^3/h]		53.7	52.4	47.6	102.2
Fuel Saving	[Nm^3/h]	-	1.3	6.1	7.5
	[%]	-	2.4	11.3	13.9

*: Heat capacity in the cited temperature intervals obtained from Figure 4.

Table 8: Energy (H) and fuel demand ($Q°_f$) for global (drying + sintering, d+r) process

	H_d [MW]	H_r [MW]	H_{d+r} [MW]	Q^0_{fd+r} [Nm^3/h]	Fuel Saving	
					[Nm^3/h]	[%]
R	1.910	0.556	2.446	238.1	-	-
RSS10	1.849	0.542	2.391	230.9	7.2	3.0
RSS20	1.753	0.492	2.246	216.9	21.2	8.9
RSS30	1.554	0.478	2.032	196.2	41.9	17.6

Table 9: CO_2 emissions from carbonates content (Carb), fuel combustion (Q^o_{fd+r}) and global process.

	Carbonates Content				Fuel Combustion				CO_2Global Emission		
	Carb [%]	CO_2 [Kg/h]	CO_2Saving		Q^0_{fd+r} [Nm^3/h]	CO_2 [Kg/h]	CO_2Saving		[Kg/h]	CO_2Saving	
			[Kg/h]	[%]			[Kg/h]	[%]		[Kg/h]	[%]
R	18.8	861.7	-	-	238.1	511.9	-	-	1373.5	-	-
RSS10	17.0	779.2	82.5	9.6	230.9	496.4	15.5	3.0	1275.5	98.0	7.1
RSS20	15.2	696.7	165.0	19.1	216.9	466.2	45.7	8.9	1162.9	210.6	15.3
RSS30	13.5	618.8	242.9	28.2	196.2	421.8	90.1	17.6	1040.5	333.0	24.2

FIGURE CAPTIONS

Figure 1: XRD patterns of bulk clay, R, and EAF-SS slag. Main phases and PDF codes are listed.

Figure 2: Thermal analyses of clay and EAF-SS slag mixtures. a) Thermal dilatometric analysis. b) Thermogravimetric analysis and c) Differential scanning calorimetry

Figure 3: Main technology properties of fired materials

Figure 4: Specific Heat, C_e, of the studied mixtures up to 950 ºC. Temperature intervals correspond to a: loss of moisture and/or water absorbed; b: oxidation of organic matter; c: de-hydroxylation of clay phyllosilicates and quartz allotropic transformation; d: decomposition of carbonates: e: formation of new crystalline phase

Figure 5: CO_2, SO_2, HCl and HF emission curves for the studied materials up to 1050 ºC.

FIGURE 1

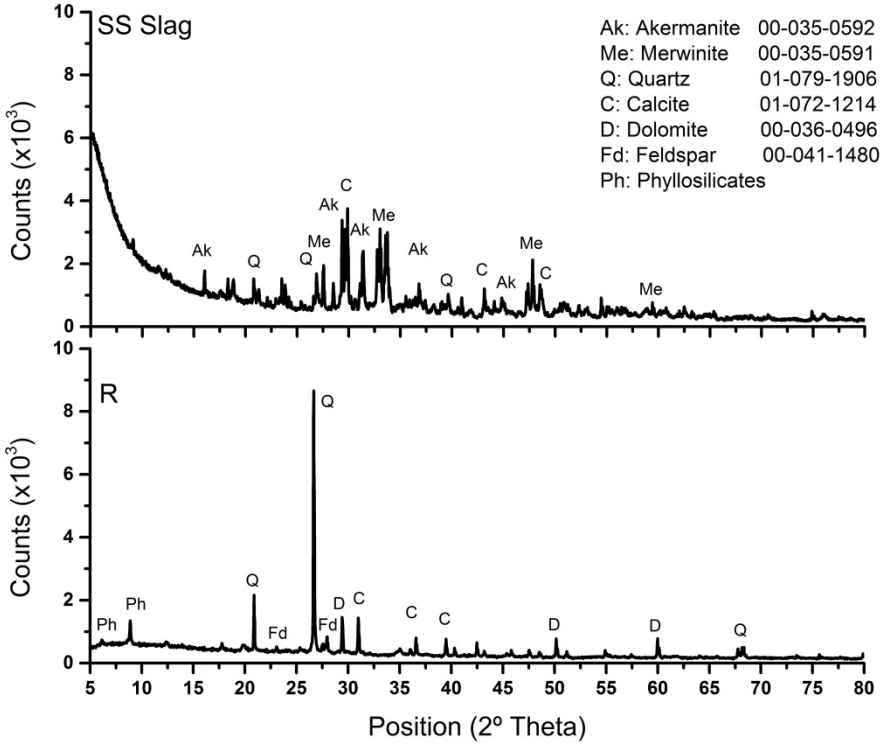
SS Slag
Ak: Akermanite 00-035-0592
Me: Merwinite 00-035-0591
Q: Quartz 01-079-1906
C: Calcite 01-072-1214
D: Dolomite 00-036-0496
Fd: Feldspar 00-041-1480
Ph: Phyllosilicates
Counts (x10^3)
R
Position (2º Theta)

FIGURE 2

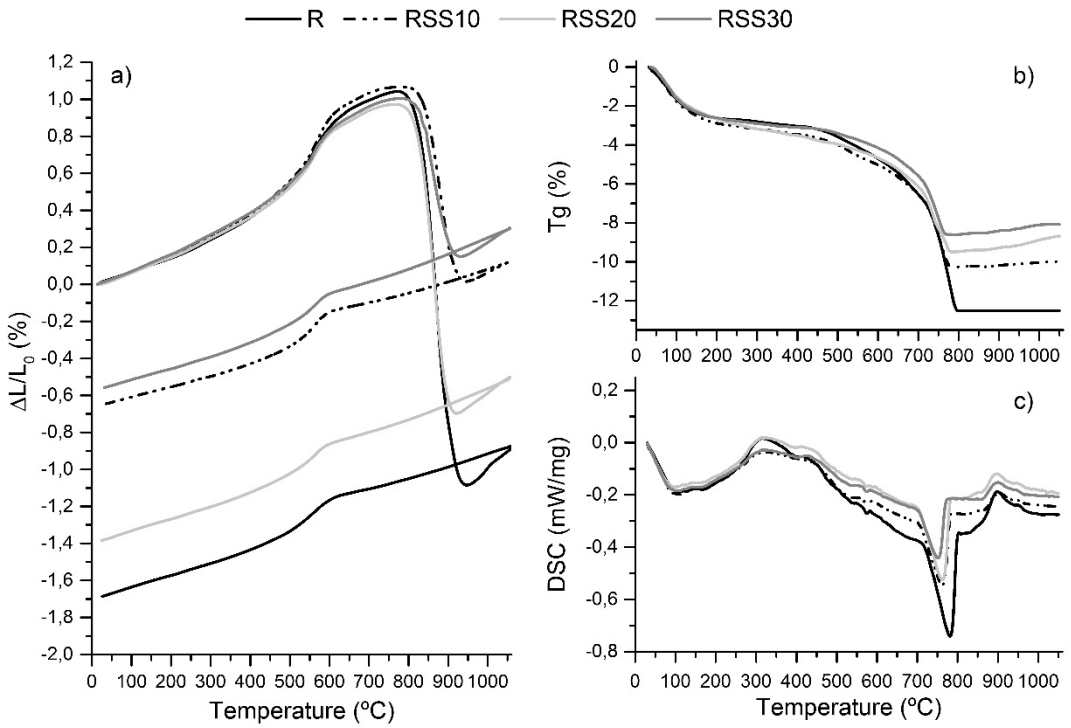
R
RSS10
RSS20
RSS30
a)
b)
c)
ΔL/L0 (%)
Tg (%)
DSC (mW/mg)
Temperature (ºC)
Temperature (ºC)

FIGURE 3

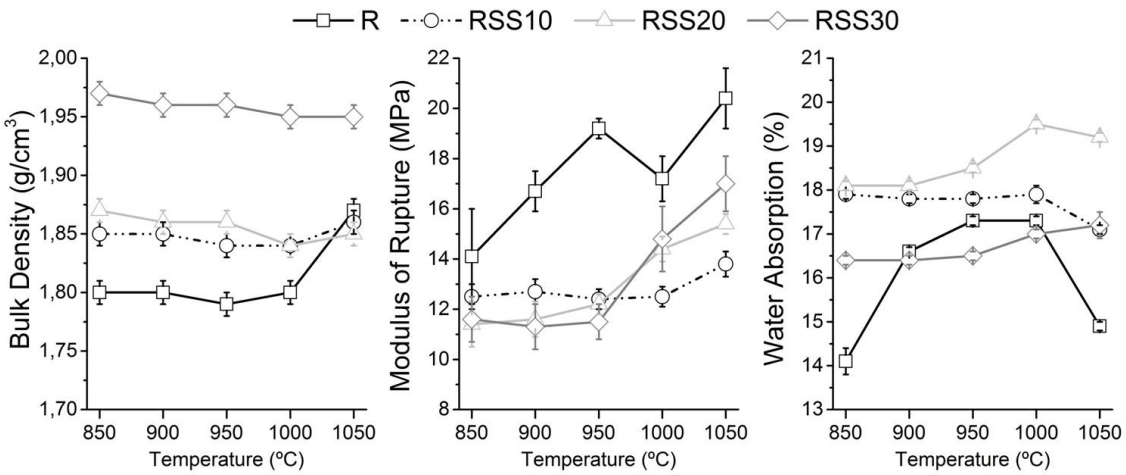
R
RSS10
RSS20
RSS30
Bulk Density (g/cm³)
Modulus of Rupture (MPa)
Water Absorption (%)
Temperature (ºC)
Temperature (ºC)
Temperature (ºC)

FIGURE 4.

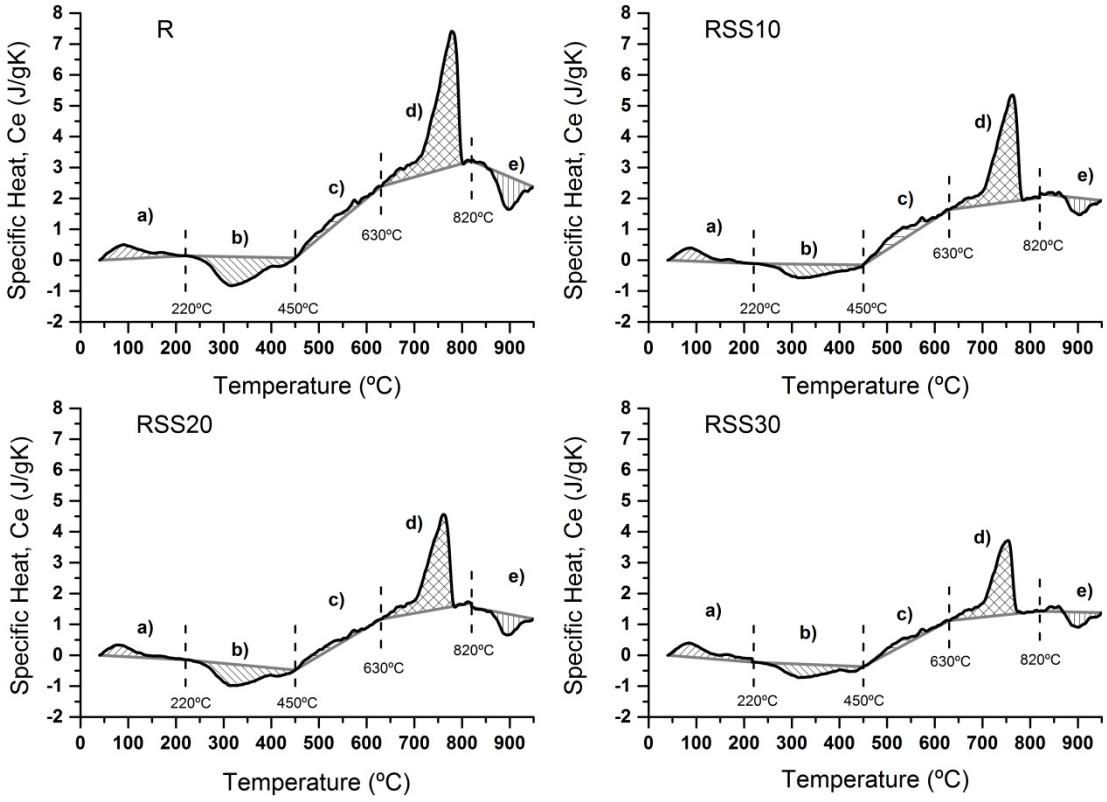
R
RSS10
RSS20
RSS30
Specific Heat, Ce (J/gK)
Temperature (ºC)
a)
b)
c)
d)
e)
220ºC
450ºC
630ºC
820ºC

FIGURE 5

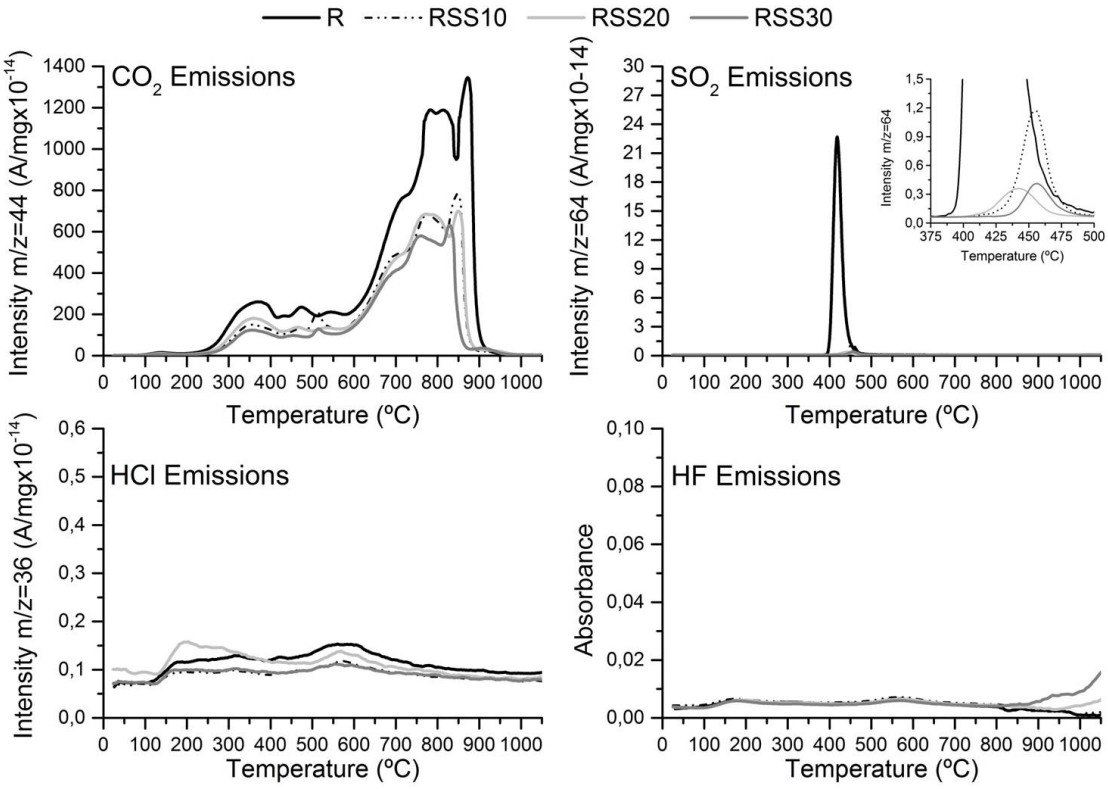
R
RSS10
RSS20
RSS30
CO2 Emissions
Intensity m/z=44 (A/mgx10-14)
Temperature (ºC)
SO2 Emissions
Intensity m/z=64 (A/mgx10-14)
Intensity m/z=64
Temperature (ºC)
HCl Emissions
Intensity m/z=36 (A/mgx10-14)
Temperature (ºC)
HF Emissions
Absorbance
Temperature (ºC)